

Sizing optimization of a thermoelectric generator set with heatsink for harvesting human body heat

Marianne Lossec*, Bernard Multon, Hamid Ben Ahmed

SATIE, ENS Cachan – Brittany Campus, CNRS, UEB, Avenue Robert Schuman, F-35170 Bruz, France

ARTICLE INFO

Article history:

Received 5 November 2011

Accepted 15 January 2013

Available online 21 February 2013

Keywords:

Energy harvesting
Thermoelectricity
Energy modeling

Heatsink
Bi-objective optimization

ABSTRACT

This paper focuses on the sizing optimization of a thermoelectric generator, combined with a potential heatsink, that harvests heat from the human body. To ensure success, energy models describing a thermoelectric module and a heatsink are introduced; these two models are then simplified for small temperature differences while respecting the continuity between them (both with and without the heatsink). In order to maximize the power produced by such a system, the dual thermal and electrical matching of the generator with its environment is studied in detail. Lastly, to optimize the sizing, a set of optimization parameters are defined, namely leg length, the capture surface area of the thermoelectric generator and, if a heatsink is present, its height. The results derived help draw a conclusion on the pertinence of adding a heatsink, for the purpose of maximizing electrical power while minimizing total volume.

© 2013 Elsevier Ltd. All rights reserved.

1. Introduction

As part of a study on multisource generator-harvesting resources within the human environment [1] (heat, light, movement), this paper focuses on the potential for thermoelectric generation from human body heat. The goal herein is to maximize thermoelectric productivity for the purpose of charging an accumulator that is capable of supplying a consumer electronic device, e.g. communicating sensor.

To this end, the thermoelectric generation [2,3] consists of placing one side of a thermoelectric module in contact with human skin and the other in direct contact with ambient air, possibly via a heatsink. The temperature difference between the two sides is then used to directly convert heat into electricity; this difference however remains relatively low, mainly as a result of the small temperature differential between the two heat sources (human body and ambient air), as well as to a poor thermal coupling of the generator with its environment [4]. The output voltage of the thermoelectric generator (TEG) thus remains fairly low. In addition, the number of thermocouples in series is limited by the integration constraints and available area. For all these reasons, a matching converter is necessary to increase the voltage as a means of connecting the generator to a storage element, in which voltage typically lies between 1 and 4 V depending on the technology introduced. Fig. 1 displays a diagram of the system under study.

The sizing of such a device should be performed according to a system-level approach that takes both the thermal coupling with

the environment and the electrical coupling with the DC–DC converter (including losses) into account. In this paper however, we will simply address the sizing of a TEG, potentially with a heatsink, not connected to a DC–DC converter. More specifically, we will focus on the sizing optimization of a TEG in terms of volume and follow this step up by presenting a method that can be extended to other criteria. The dual thermal and electrical matching for maximized energy harvesting will also be studied.

2. Thermoelectric system modeling

In order to optimize the sizing of a TEG with a potential heatsink, generic sizing models, based on existing technologies, must first be established. The application studied herein involves harvesting heat from the human body, though the models presented are easily transposable to other applications.

2.1. Thermal and electrical models of a thermoelectric generator (TEG)

In the particular context of harvesting energy from the human body, the thermal TEG model, as simplified for small temperature differences, is shown in Fig. 2. The Joule losses and heat flow due to the Seebeck effect can both be considered negligible, in comparison with the main heat flow. This assumption has been justified in [4].

The distinctive features of such a system within the human environment are the very limited amount of resources available and the poor thermal coupling with the environment, thus resulting in a small effective difference in temperature between hot and cold heat sources. Given the level of recoverable power, the human

* Corresponding author. Tel.: +33 (0)299059322.

E-mail address: marianne.lossec@bretagne.ens-cachan.fr (M. Lossec).

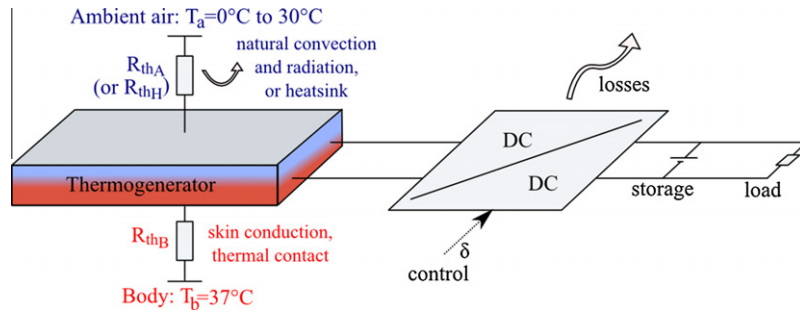


Fig. 1. Thermoelectric generation system using the human body.

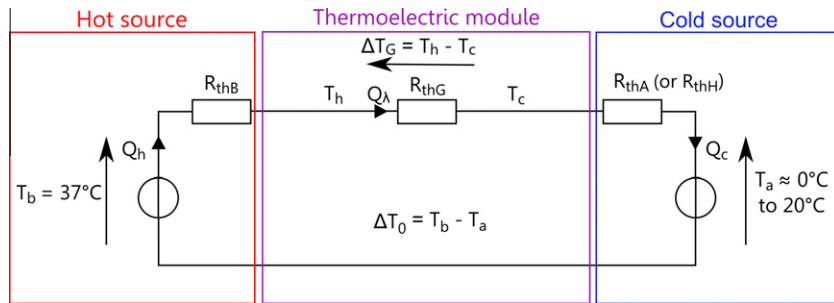


Fig. 2. Simplified thermal model of the TEG.

body and its environment can be considered as “infinite sources of temperature”, i.e. unaffected by the presence of the TEG. Couplings of the hot and cold sides with temperatures T_b and T_a are represented by two thermal resistances R_{thB} and R_{thA} , with R_{thB} being the thermal resistance between the hot heat source (the human body in this case) and the hot side of the module. The value of R_{thB} equals the sum of the thermal conduction resistance of both the human skin and the thermal contact between the skin surface and the hot side of the module. For its part, R_{thA} is the thermal resistance between the cold side of the module and the surrounding air; it corresponds to radiation and natural convection of the cold side with ambient air and is very sensitive to both position and movements. Note that a pin fin heatsink can also be added to improve heat transfer, but this would increase the overall volume. In this case, we denote R_{thH} as the thermal resistance of the heatsink. In addition to these two resistances, the thermal resistance R_{thG} represents heat conduction through all N_{th} thermocouples, which are thermally connected in parallel and constitute the TEG. Lastly, ΔT_0 denotes the temperature difference between the hot source T_b and cold source T_a , with the temperature difference ΔT_G on the TEG thermal surfaces being expressed as:

$$\Delta T_G = \frac{R_{thG}}{R_{thG} + R_{thB} + R_{thA}} \Delta T_0 \quad (1)$$

From a purely electrical standpoint, the N_{th} thermocouples are electrically connected in series and therefore display a total electrical resistance denoted R_G . The TEG thus behaves like an electromotive force (emf) E_G (proportional to both ΔT_G and the Seebeck coefficient α), associated with an internal resistance R_G (Fig. 3). Note that $\alpha = N_{th} * \alpha_0$, with α_0 representing the Seebeck coefficient of a thermocouple.

In considering the notations indicated in Fig. 4, as denoted ρ and λ respectively for the electrical resistivity and thermal conductivity of a thermocouple (average of the two materials), h_A and h_B the heat transfer coefficients on both sides of the TEG, and k_f the filling factor of thermocouples in the TEG, we can now express the thermal and electrical resistances previously defined by:

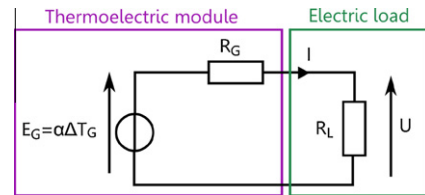


Fig. 3. Electrical model of the TEG.

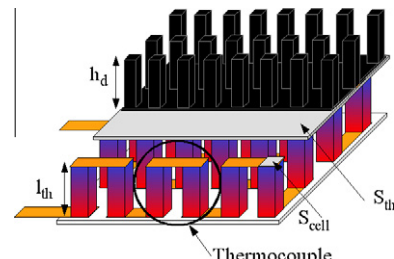


Fig. 4. Indications of the TEG notations.

$$R_{thB} = \frac{1}{h_B S_{th}}; \quad R_{thG} = \frac{l_{th}}{2k_f S_{th}} \\ R_{thA} = \frac{1}{h_A S_{th}}; \quad R_G = N_{th}^2 \rho \frac{4l_{th}}{k_f S_{th}} \quad (2)$$

Regardless of the electrical load R_L connected to the TEG, the recoverable electrical power P_e can thus be expressed as follows:

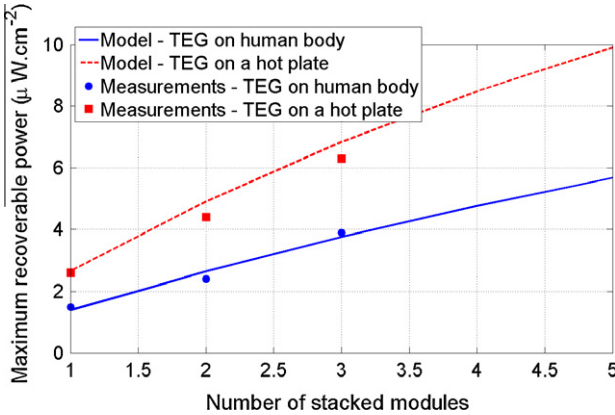
$$P_e = \frac{k_c E_G^2}{R_G} = \frac{k_c (\alpha \Delta T_G)^2}{R_G} \quad (3)$$

The coefficient k_c depends on the electrical operating point of the TEG and lies between $0 \leq k_c \leq \frac{1}{4}$. For a perfect electrical impedance matching, the coefficient value equals $\frac{1}{4}$, in which case the electrical power is maximized [5,6]; this maximum power is denoted P_{eM} .

Table 1

Parameter values associated with TEG and its environment.

N_{th}	450	S_{th}	30 cm ²
α_0	267 $\mu\text{V K}^{-1}$	l_{th}	1.5 mm
λ	0.77 W m ⁻¹ K ⁻¹	T_a	22 °C
ρ	20 $\mu\Omega \text{m}$	T_b	37 °C
k_f	0.6	h_A	13 W m ⁻² K ⁻¹
k_c	0.25	h_B	25 W m ⁻² K ⁻¹

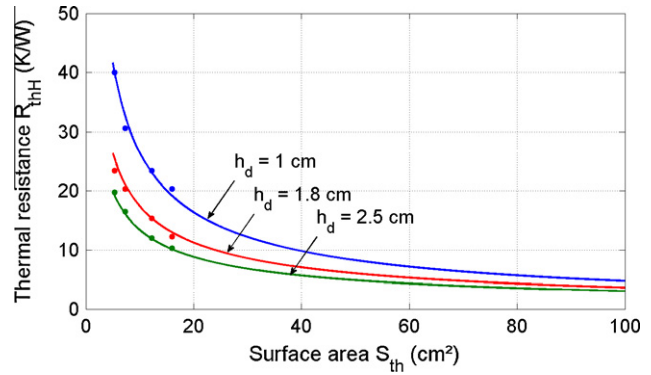
**Fig. 5.** Evolution of the maximum recoverable power in both measured data (dots and squares) and theoretical data (solid and dashed lines) vs. the number of stacked modules.

These benchmark models have been validated from experiments performed using the thermoelectric module TM-450-0.8-3.0 produced by the Ferrotec company. This module contains $N_{th} = 450$ bismuth telluride thermocouples, for a total surface area of approx. $S_{th} = 30 \text{ cm}^2$ and a leg length of $l_{th} = 1.5 \text{ mm}$. Experiments were conducted at an ambient temperature of $T_a = 22 \text{ }^\circ\text{C}$ for various cases. First, the TEG was placed on a hot plate at $T_b = 36 \text{ }^\circ\text{C}$ in considering a perfect contact between the TEG and the hot plate ($R_{thB} = 0$). Next, the TEG was placed in direct contact with the skin of a human being (imperfect flatness). Moreover, a solution to improve energy harvesting, with a given a surface area, consists of stacking identical thermoelectric modules and connecting them electrically in series [3,4]. For the current experimental campaign, one, two or three thermoelectric modules were therefore stacked. The stacking of thermoelectric modules ultimately amounts to increasing the leg length l_{th} of the TEG, in the case where the effects of a module's alumina plates are neglected and only a one-way heat flow is considered. It was also assumed that the contact between two stacked modules is perfect, which implies that the electrical and thermal contact resistances, as well as the device substrate thermal resistances, can be neglected. This assumption was made due to the inability of identifying the given resistances. The consequence of such an assumption therefore is that the thermal resistance of the TEG R_{thG} is overestimated as the leg length increases.

By taking into account the values listed in Table 1, Fig. 5 shows the maximum recoverable power vs. the number of stacked modules. The dots and squares in this figure correspond to measured data, while the solid and dashed lines depict the model dataset.

2.2. Heatsink model

Adding a heatsink to this set-up enhances the thermal coupling between the cold side of the TEG and ambient air [7]. The thermal resistance of this heatsink R_{thH} depends on its total exchange surface area S_{th_tot} , which itself depends on its associated capture surface area S_{th} and height h_d (Fig. 4). S_{th_tot} actually corresponds to

**Fig. 6.** Thermal model of the heatsink.**Table 2**

Parameter values for the heatsink model.

k_{H1}	19.5 W m ⁻² K ⁻¹
k_{H2}	0.67

both the outer exchange surface area S_{out} (i.e. perimeter of the heatsink multiplied by its height) and the inner exchange surface area S_{in} , which is proportional to S_{th} . In denoting k_{H1} and k_{H2} as two constant coefficients describing the heatsink technology, the model can now be expressed as follows:

$$R_{thH} = \frac{1}{k_{H1} S_{th_tot}} = \frac{1}{k_{H1} (S_{out} + S_{in})} = \frac{1}{k_{H1} (4h_d \sqrt{S_{th}} + k_{H2} S_{th})} \quad (4)$$

We examined the heatsink datasheets provided by the Aavid company in order to build a thermal model. The fin geometry of such a heatsink is shown in the design diagram in Fig. 4. Fig. 6 presents, for various fin heights h_d , the variation in R_{thH} vs. surface area S_{th} . The dots correspond to values listed on the datasheet, while the solid lines refer to the model dataset, with the values of k_{H1} and k_{H2} defined in Table 2. (Note: This model has been extrapolated since the max. surface area of the heatsinks produced by Aavid is only 16 cm².)

Let us note that model continuity has been preserved. When the heatsink height h_d equals zero, the thermal resistance R_{thH} indeed equals the thermal resistance R_{thA} , which corresponds to radiation and natural convection, i.e. $h_A = k_{H1} * k_{H2}$.

3. Maximizing the electrical power of the TEG

According to the classical maximization step of thermoelectric power theory [2], heat flow through the TEG is assumed to be constant so that maximizing TEG efficiency (i.e. ratio of electrical power to the heat flow collected at the hot source) is equivalent to maximizing electrical power. This hypothesis however is not applicable to our study since heat flow has not been imposed. Maximizing the recovered electrical power [8,9] must then be treated as a different problem from that of maximizing efficiency, by use of more appropriate means.

3.1. Thermal impedance matching

The thermal and electrical models presented above, in association with the heatsink model, enable us to express the emf E_G and electrical power P_e of the TEG as follows:

$$E_G = N_{th} \alpha_0 \Delta T_0 \frac{l_{th}}{l_{th} + k_{env}} \quad (5)$$

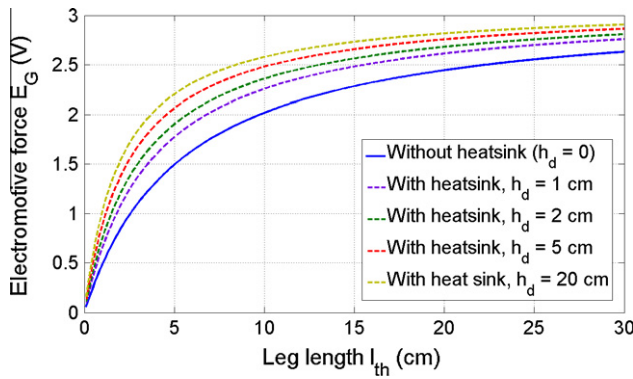


Fig. 7. Evolution of emf E_G vs. leg length l_{th} , both with and without a heatsink.

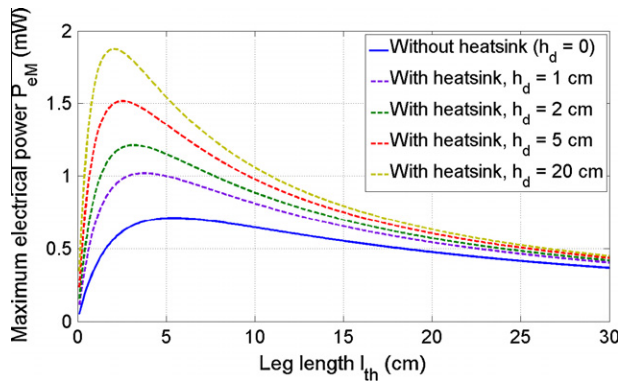


Fig. 8. Evolution of power P_{eM} vs. leg length l_{th} , both with and without a heatsink.

$$P_e = \frac{k_c k_f \alpha_0^2 \Delta T_0^2}{4\rho} \frac{S_{th} l_{th}}{(l_{th} + k_{env})^2} \quad (6)$$

The value of coefficient k_{env} depends on the height of the heatsink, whereby a zero value corresponds to a TEG without a heatsink. This coefficient is expressed below in taking into account the previous thermal models:

$$k_{env} = \lambda k_f \left(\frac{1}{h_B} + \frac{1}{k_{H1} \left(\frac{4h_d}{\sqrt{S_{th}}} + k_{H2} \right)} \right) \quad (7)$$

By inputting the parameter values listed in Tables 1 and 2, Figs. 7 and 8 show respectively the evolution of emf E_G and electrical power P_{eM} on the adapted load ($k_c = 1/4$), both with and without a heatsink (i.e. $h_d = 0$), as a function of the leg length l_{th} .

Given a surface area S_{th} and leg length l_{th} , the addition of a heatsink can enhance the emf E_G as well as the electrical power P_{eM} . The shape of P_{eM} is known [10] and exhibits an optimum value for leg length as a ratio of heatsink height, though this optimal length tends to be technologically infeasible (i.e. too high). One approach to achieving basically the same improvement would be to stack the modules, as pointed out above.

A fundamental problem of harvesting energy from the human body relates to the poor thermal matching of a TEG with its environment. In other words, the thermal resistance R_{thG} is generally very low compared to the environment-related resistances R_{thB} and R_{thA} (or R_{thH} with a heatsink). Let us denote R_{thE} as the sum of thermal resistances related to the environment, i.e. $R_{thB} + R_{thA}$ without a heatsink and $R_{thB} + R_{thH}$ with a heatsink. Since the internal thermal and electrical resistances of the TEG, denoted respectively R_{thG} and R_G , are proportional to the leg length l_{th} , an increase in leg length serves to improve the thermal coupling

and thus increases ΔT_G , yet also enhances the internal resistance R_G and therefore *a priori* decreases the maximum electrical power harvested. In considering Eq. (6), it is possible to prove that electrical power is maximized for an optimal value of l_{th} [11], which depends on heatsink height and thus differs whether or not the heatsink is present. This condition is expressed as follows:

$$l_{thopt} = \lambda k_f \left(\frac{1}{h_B} + \frac{1}{k_{H1} \left(\frac{4h_d}{\sqrt{S_{th}}} + k_{H2} \right)} \right) \quad (8)$$

The maximum power is obtained when the internal thermal resistance of TEG R_{thG} equals the sum of thermal resistances in its environment, i.e. summing to R_{thE} . The difference in temperature ΔT_G across the TEG is thus equal to half the difference in temperature between the body and ambient air [12], a situation that corresponds to thermal impedance matching.

Increasing the leg length (or stacking thermoelectric modules) thus improves thermal coupling for a given surface area, which in turn increases the emf and electrical power of the TEG. This result proves to be a considerable advantage when connecting the TEG to a DC-DC converter. At these power levels, major losses in the converter are in fact switching losses that decrease as input voltage increases [13]. The best solution to reduce these losses would be to include a high number of thermocouples in the TEG; for example, the TEG produced by the Micropelt and Thermolife companies are made of a thin film. This technology allows integrating a greater thermocouple density (approx. 5000 per cm^2 compared to 15 per cm^2 for the module TM-450-0.8-3.0 produced by the Ferrotec company) and therefore yields high open circuit voltages E_G of TEGs relative to the surface area of the hot/cold plate. The solution discussed above of stacking modules also offers a way to increase E_G when the leg length is limited for technological reasons.

Increasing the leg length and/or adding a heatsink however also expands the size, i.e. volume, of the TEG, which can now be expressed as:

$$V_{th} = S_{th} (l_{th} + h_d) \quad (9)$$

As a result, it may be worthwhile to size the TEG by seeking to minimize volume while maximizing energy recovery; this approach will be discussed further below.

3.2. System sizing optimization

In order to size a TEG that maximizes the electrical power produced while minimizing its volume, we have introduced a bi-objective multi-variable optimization algorithm based on particle swarm optimization [14] and Pareto dominance. This algorithm, called MOPSO, has been implemented in a Matlab environment in our laboratory and has already been used for another application [15]. We were thus able to optimize TEG sizing, both with and without a heatsink, in considering electrical impedance matching (i.e. the TEG voltage is thus equal to half its emf). With a given number of optimization parameters (here S_{th} , l_{th} and h_d if a heatsink is present), this optimization algorithm returned, after several iterations, a set of optimal solutions meeting the input specifications and distributed on a Pareto front. The two competing criteria chosen are: minimization of the TEG and heatsink (if present) volume V_{th} ; and maximization of harvested electrical power P_{eM} . In addition, we forced the geometric parameters to vary only within a bounded interval (see Table 3). Note that the constraint introduced to limit heatsink height to 10 cm is arbitrary, but it was necessary to set a limit in order to respect the validity of this thermal resistance model. For these optimizations, the temperature values of the body (T_b) and ambient air (T_a) are those listed in Table 1. Moreover, a constant thermocouple density, equal to that of module TM-450-0.8-3.0

Table 3

Bounded interval of the geometric parameters for the optimization algorithm.

Parameter	Min	Max
S_{th}	0	100 cm ²
l_{th}	0	10 cm
h_d	0	10 cm

(Ferrotec), was assumed due to a lack of sufficient generic information on the effects of thermocouple density. The number of thermocouples N_{th} is thus proportional to the surface area S_{th} . Lastly, let us recall that it was decided to vary the leg length, which is roughly equivalent to stacking modules (with an exception made for the thickness of the modules' alumina plates).

Fig. 9 shows the Pareto front solutions of optimizations with volume minimization and power maximization. The red dots correspond to the optimization of a TEG with a heatsink, while the blue dots reflect the TEG optimization without a heatsink. For this second optimization, we forced the value of parameter h_d , which corresponds to heatsink height, to zero, i.e. $h_d = 0$.

It can be noticed that the two Pareto fronts obtained overlap at first. Then, beyond the coordinate point $V_{th} = 120 \text{ cm}^3$ and $P_{eM} = 0.8 \text{ mW}$, the effect of adding a heatsink, given a certain volume, makes it possible to harvest greater power.

As a preferred approach to interpreting these results, we studied the evolution in optimization parameters, i.e. surface area S_{th} (Fig. 10), leg length l_{th} and heatsink height h_d (Fig. 11), as well as the evolution in thermal resistances of both the generator R_{thG} and the environment R_{thE} (Fig. 12).

For the sizing optimization of a TEG that harvests maximum power as a result of electrical impedance matching, let us observe

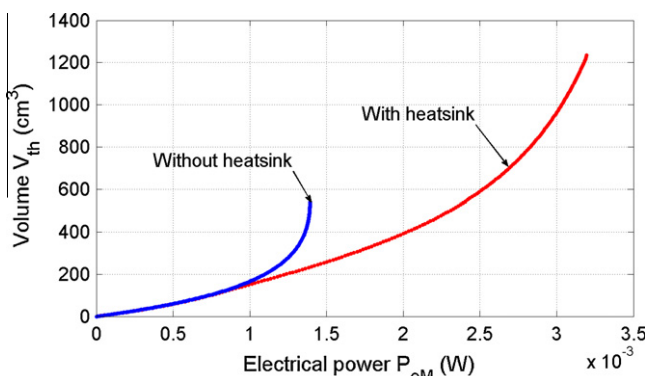


Fig. 9. Bi-objective optimization solutions that minimize volume and maximize productivity.

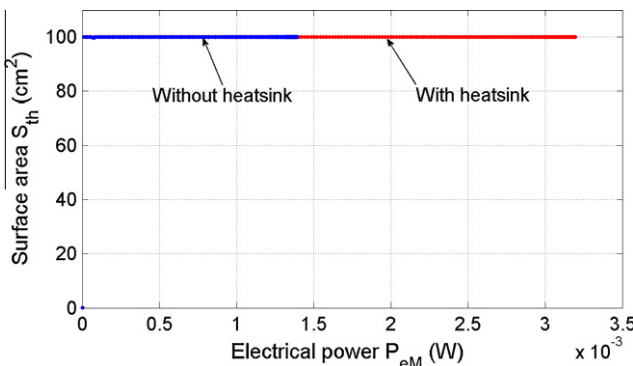


Fig. 10. Evolution in the optimal surface area S_{th} vs. electrical power P_{eM} .

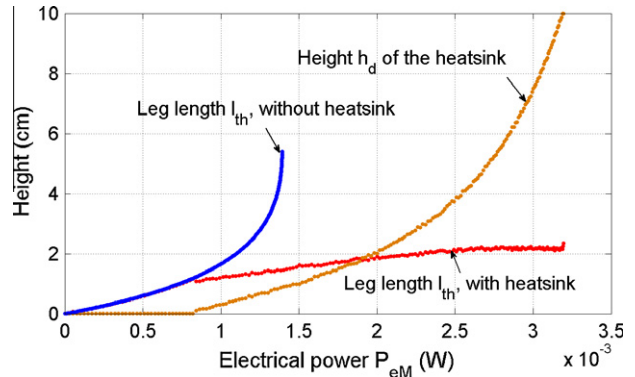


Fig. 11. Evolution in the optimal leg length l_{th} and heatsink height h_d vs. electrical power P_{eM} .

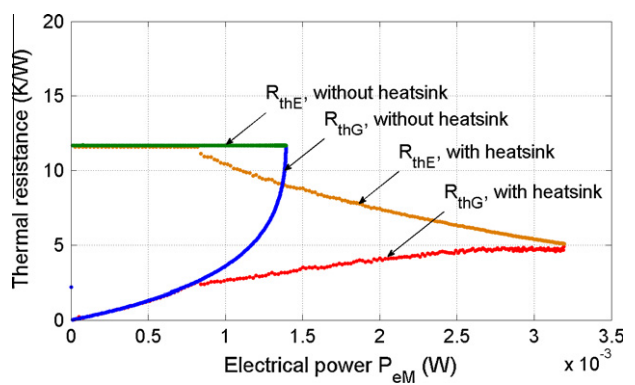


Fig. 12. Evolution in thermal resistances, R_{thG} and R_{thE} , vs. electrical power P_{eM} .

that without the presence of a heatsink, the surface area S_{th} chosen by the optimization algorithm is always the maximum allowed, i.e. here 100 cm^2 (blue dots in Fig. 10). According to Eqs. (6) and (7), regardless of the electrical operating point of the TEG, its power is always proportional to S_{th} . Hence, in order to increase the harvested power with a given surface area, the leg length l_{th} must simply be increased to its optimum value (see Eq. (8)). In Fig. 11, the evolution of l_{th} without a heatsink basically corresponds to the increasing part of the P_{eM} vs. l_{th} graph, as plotted in blue¹ in Fig. 8. Once the maximum power has been reached, the increase in l_{th} is no longer beneficial. For a desired electrical power and given heat exchange conditions, it then becomes preferable to introduce large surface areas and a thin TEG. Moreover, in Fig. 12, the evolution in thermal resistances of both the generator R_{thG} and environment R_{thE} confirms that maximum power is achieved for a satisfactory thermal impedance matching, i.e. when $R_{thG} = R_{thE}$.

For the sizing optimization of a TEG including a heatsink, the electrical power is no longer proportional to surface area S_{th} given that coefficient k_{env} depends on S_{th} , as a result of the heatsink model (Eq. (7)). The value of S_{th} selected by the algorithm (red dots in Fig. 10) however remains the maximum allowed. Regarding the evolution of l_{th} and h_d , Fig. 11 shows that at low power levels, the heatsink height h_d equals zero, which means that adding a heatsink is not advantageous. Thanks to the continuity of the heatsink model (Eq. (4)), the two Pareto fronts illustrated in Fig. 9 can thus be combined. Fig. 11 also shows that at higher power, the TEG with a heatsink height greater than the leg length is to be preferred. In addition, it has been observed that the power attained

¹ Please note that Figs. 8 and 10 will appear in B/W in print and color in the web version. Based on this, please approve the footnote 1 which explains this.

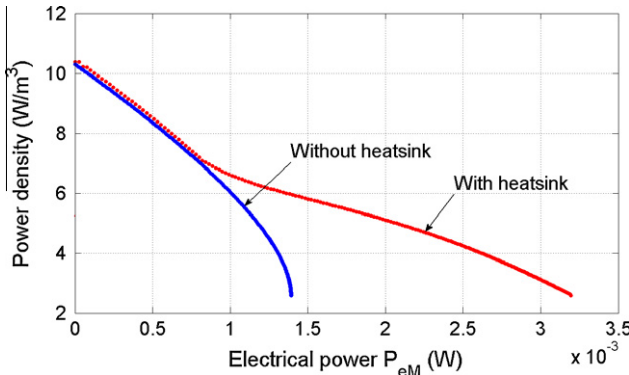


Fig. 13. Evolution in power density vs. electrical power.

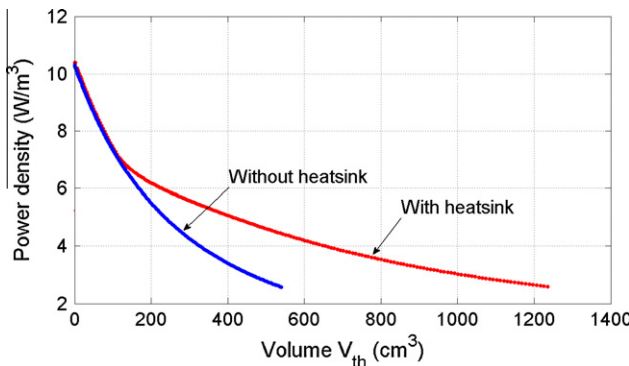


Fig. 14. Evolution in power density vs. volume.

is higher when adding a heatsink, since power increases with heatsink height h_d (Eqs. (6) and (7)). Maximum power is actually attained by the algorithm when the heatsink height equals the maximum allowed value, i.e. 10 cm (Fig. 11). Lastly, thermal impedance matching has been observed for a TEG with a heatsink when electrical power is maximized (Fig. 12).

In Figs. 13 and 14, the power density (i.e. power per unit volume) has been plotted vs. both electrical power and volume, respectively.

Let us note in Figs. 13 and 14 that whether with or without a heatsink, volume increases faster than electrical power (i.e. the power density function is decreasing).

Furthermore, these optimizations could be conducted by setting power density maximization as the optimization criterion rather than electrical power maximization. We opted for this approach and found the same results as presented above.

4. Conclusion

In this paper, we have presented the sizing optimization, in terms of volume, of a thermoelectric generator, which as an option may include a heatsink, in the specific context of harvesting energy from the human body.

Models of a thermometric module, simplified for small temperature differences, and a heatsink were built from experimental validation or datasheets, and both types of models were based on existing technologies. Moreover, continuity between the two models has been well respected, meaning that for a given surface area the thermal resistance of a heatsink with zero height corresponds to the radiation and natural convection resistance of the thermoelectric module. This study of TEG, with or without a heatsink, highlights the relevance of electrical and thermal matching of the TEG to its environment in order to maximize its power. Thermal

impedance matching can be performed by increasing the TEG leg length until its optimum value or, should this prove technologically infeasible, by stacking thermoelectric modules.

The models developed models have enabled the sizing optimization of such a thermoelectric generator. By defining two competing optimization criteria, consisting of minimizing the TEG volume (with the inclusion of a potential heatsink) while maximizing the power produced by the generator, we have demonstrated that from a certain volume, adding a heatsink makes it possible to harvest more power. Moreover, we have shown that the solution minimizing volume leads to an ultra-thin TEG with power being maximized when TEG impedance is matched thermally and electrically with its environment. If the capture surface area is indeed limited, then the minimization of total volume yields a greater thermocouple leg length (e.g. by stacking modules). Under these conditions, maximum electrical power is obtained for a leg length corresponding to thermal matching (equality between the TEG thermal resistance and the thermal resistance related to the environment). At higher electrical power, a heatsink is necessary to improve thermal coupling with the environment, and the total volume is still minimized for a leg length (smaller this time) leading to thermal matching with a heatsink.

Furthermore, the TEG studied herein displays a low thermocouple density. Technologies using higher density (though *a priori* theoretically less productive per unit area) could be better suited to such a system optimization. It might prove beneficial to define thermocouple density as an optimization parameter.

To the best of our knowledge, such global optimization results are entirely new, with this method being potentially extended to other criteria as well, i.e. economic or environmental, provided a sufficient amount of data has been associated with these criteria.

References

- [1] M. Lossec, B. Multon, H. Ben Ahmed, L. L'Hours, P. Quinton, J. Prioux et al., Optimization methodology for a multi-source-energy generation system using the human environment energy resource, in: New Electrical Systems in Tours, May 2008.
- [2] Rowe DM. CRC handbook of thermoelectrics. London: CRC Press; 1995.
- [3] Leonov V, Torfs T, Fiorini P, Van Hoof C. Thermoelectric converters of human warmth for self-powered wireless sensor nodes. *IEEE Sens J* 2007;7:650.
- [4] Lossec M, Multon B, Ben Ahmed H, Goupil C. Thermoelectric generator placed on the human body: system modeling and energy conversion. *EPJAP* 2010;52:11103.
- [5] Chuang Yu, Chau KT. Thermoelectric automotive waste heat energy recovery using maximum power point tracking. *Energy Convers Manage* 2009;50:1506–12.
- [6] Zhang Xiaodong, Chau KT. An automotive thermoelectric–photovoltaic hybrid energy system using maximum power point tracking. *Energy Convers Manage* 2011;52:641–7.
- [7] Siivola E, Mahadevan R, Crocco P, Von Gunten K, Koester D. Design considerations for TEG system optimization. Nextreme Thermal Solutions Inc. Whitepaper; 2010.
- [8] Rowe JDM, Min G. Design theory of thermoelectric modules for electrical power generation. *IEE Sci Measure Technol* 1996;143:351–6.
- [9] T. Hendricks, W.T. Choate, Engineering scoping study of thermoelectric generator systems for industrial waste heat recovery, U.S. Department of Energy; 2006.
- [10] Stevens JW. Optimal design of small ΔT thermoelectric generation systems. *Energy Convers Manage* 2001;42:709–20.
- [11] Glatz W, Muntwyler S, Hierold C. Optimization and fabrication of thick flexible polymer based microthermoelectric generator. *Sensor Actuat A* 2006;132:337–45.
- [12] V. Leonov, P. Fiorini, Thermal matching of a thermoelectric energy scavenger with the ambiance, in: European conference on thermoelectrics; 2007, p. 129–33.
- [13] M. Lossec, B. Multon, H. Ben Ahmed, Sizing optimization with thermal and electrical matching of a thermogenerator placed on the human body, in: International conference on renewable energy and eco-design in electrical engineering, March 2011.
- [14] Reyes-Sierra M, Coello Coello CA. Multi-objective particle swarm optimizers: a survey of the state-of-the-art. *Int J Comput Intell Res* 2006;2(3):287–308.
- [15] Aubry J, Ben Ahmed H, Multon B. Sizing optimization methodology of a surface permanent magnet machine-converter system over a torque-speed operating profile: application to a wave energy converter. *IEEE Trans Ind Electron* 2011.